Electromagnetically induced blazed grating at low light levels

Silvânia A. Carvalho and Luís E. E. de Araujo*

Instituto de Física "Gleb Wataghin," Universidade Estadual de Campinas, 13083-859 Campinas, São Paulo, Brazil

(Received 11 February 2011; published 18 May 2011)

We propose a scheme for inducing a blazed transmission grating in a four-level, N-type atomic medium under electromagnetically induced transparency (EIT). The blazed grating relies on the giant Kerr nonlinearity that the atomic medium exhibits under EIT. The grating is created using an intensity mask in one of the driving optical fields and only weak fields with intensities below saturation level are involved. Diffraction efficiencies of a resonant probe beam close to 100% are predicted.

DOI: 10.1103/PhysRevA.83.053825 PACS number(s): 42.50.Gy, 42.65.−k

I. INTRODUCTION

A diffraction grating can be induced in an atomic vapor by introducing a spatial modulation to the atomic susceptibility. Several applications have been proposed and demonstrated experimentally for such atomic gratings: all-optical switching and routing [1], tunable photonic band gaps [2], light storage [3,4], and beam splitting and fanning [5], among others. Many of the different schemes that have been proposed for creating an atomic grating use electromagnetically induced transparency (EIT) [6]. Under EIT, a three-level Λ-type atomic sample is made transparent to a resonant probe field by means of a coupling field acting on the linked transition. By spatially modulating the coupling field using, for example, two coupling beams intersecting at an angle, regions of high and low transmission are created that are equivalent to an amplitude transmission grating on which the probe beam can diffract [7,8]. As with any amplitude grating, the first-order diffraction efficiency of such an atomic grating is low (<10%).

Phase gratings, however, are much more efficient [9]. An atomic phase grating can be created by modulating the refractive component of the atomic susceptibility instead of its absorptive component. One of the present authors recently proposed that in a four-level N-type atom, an atomic phase grating can be created by modulating not the coupling beam, but a third weak-signal beam [10]. The signal beam disrupts the EIT condition, generating a giant Kerr-type nonlinearity in the atom while simultaneously keeping probe absorption low [11]. Modulating the signal field introduces a modulation to the cross-phase-modulation (XPM) phase shift between probe and signal fields. Higher diffraction efficiencies into the first order (≈30%), approaching those of an ideal sinusoidal phase grating, were predicted [10]. A phase grating can also be induced in an atomic medium by modulating a weak microwave field applied to a double dark-state system [12]. These phase gratings, however, generate many diffraction orders, limiting the diffraction efficiency obtainable at any one of the orders. We showed recently that the first-order diffraction efficiency of the N-type atomic grating can be increased significantly (to over 70%) by having the probe beam impinge on the grating at a Bragg angle [13]. Alternatively, a blazed atomic grating, with near unity efficiency, can be created in a three-level atom by using intensity-modulated images applied to a strong-coupling field [5].

Here we describe a blazed atomic grating that combines the approaches of Refs. [5,10]. We derive an analytical expression for the grating's diffraction efficiency as a function of the atomic excitation parameters (signal detuning and Rabi frequency) as well as the probe's angle of incidence and the optical depth of the atomic sample. The proposed blazed grating is capable of diffracting a resonant probe beam into the first diffraction order with almost 100% efficiency. In contrast to the blazed grating of Ref. [5], our grating is created with only weak fields whose intensities are below the saturation intensity of the relevant atomic transitions.

II. MODEL ATOMIC SYSTEM FOR GIANT XPM

Our model atomic system consists of an N-type four-level atom interacting with three laser fields, as illustrated in Fig. 1. The excited states decay spontaneously at rates $\gamma_3 = \gamma_4$ to outside the atomic system. The ground states decay at a rate γ_0. The $|1\rangle \rightarrow |3\rangle$ transition is excited by a resonant probe beam with Rabi frequency Ω_p. The coupling beam, with Rabi frequency Ω_c, resonantly connects the ground state $|2\rangle$ to the excited state $|3\rangle$; the $|2\rangle \rightarrow |4\rangle$ transition is driven by the signal field, whose Rabi frequency is Ω_s. The signal field is far detuned from resonance by $\delta = \omega_{24} - \omega$, where ω_{24} is the atomic transition frequency and ω is the signal optical frequency.

The Λ EIT system is formed by levels $|1\rangle$, $|2\rangle$, and $|3\rangle$ together with the probe and coupling fields. The weak-signal field causes an ac Stark shift of level $|2\rangle$ and modifies the two-photon detuning between the probe and coupling fields. Due to the increased steepness of the probe dispersion under EIT [6], a small change in the two-photon detuning drastically changes the index of refraction at the probe frequency. A giant XPM nonlinearity arises between the signal and probe fields [6,11].

The equations of motion for the probability amplitudes of the atomic states are

$$\begin{aligned} \dot{a}_1 &= -\Gamma_0 a_1 + \tfrac{1}{2} i \Omega_p a_3, \\ \dot{a}_2 &= -\Gamma_0 a_2 + \tfrac{1}{2} i \Omega_c a_3 + \tfrac{1}{2} i \Omega_s a_4, \\ \dot{a}_3 &= -\Gamma_3 a_3 + \tfrac{1}{2} i \Omega_p a_1 + \tfrac{1}{2} i \Omega_c a_2, \\ \dot{a}_4 &= -\Gamma_4 a_4 + \tfrac{1}{2} i \Omega_s a_2, \end{aligned} \tag{1}$$

*araujo@ifi.unicamp.br

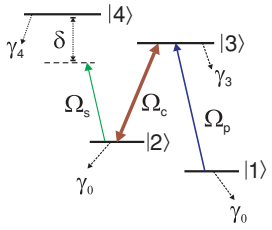

FIG. 1. (Color online) Energy-level diagram of the four-level N-type atomic system driven by three weak optical fields: probe Ω_p, coupling Ω_c, and signal Ω_s.

where $\Omega_p = 2d_{13}E_p/\hbar$, $\Omega_c = 2d_{23}E_c/\hbar$, and $\Omega_s = 2d_{24}E_s/\hbar$ are real Rabi frequencies; we also define $\Gamma_3 = \gamma_3/2$, $\Gamma_4 = \gamma_4/2 + i\delta$, and $\Gamma_0 = \gamma_0/2$. Although a wave-function model does not allow the inclusion of pure dephasing mechanisms between the ground states, it is known that such a model can mimic dephasing satisfactorily through γ_0 [6]. For large signal detunings ($\delta \gg \gamma_4$) we can ignore any increase of the ground-state decoherence rate Γ_0 due to the signal field [14]. The probe field is assumed to be so weak ($\Omega_p \ll \gamma_3$) that the atomic population stays in the ground state $|1\rangle$, while levels $|2\rangle$, $|3\rangle$, and $|4\rangle$ remain empty. We will consider the case of a homogeneously broadened system. Accordingly, the theory to be developed here is valid for cold atoms in a magneto-optical trap or atoms in a vapor cell in which collisions with a buffer gas provide a strong, homogeneous broadening of the transitions.

We solve Eqs. (1) in the steady-state regime to find the induced atomic polarization at the probe frequency $P_{13} = nd_{13}a_1^*a_3$, where n is the atomic density. Writing $P_{13} = \epsilon_0\chi E_p$, where χ is the atomic susceptibility and E_p is the probe's electric-field amplitude, we find to first order in the probe field

$$\begin{aligned} \mathrm{Re}(\chi) &= \left(2nd_{13}^2/\hbar\epsilon_0\right)\frac{2(\Omega_s/\Omega_c)^2\delta}{4\delta^2 + [\gamma_4 + \gamma_3(\Omega_s/\Omega_c)^2]^2}, \\ \mathrm{Im}(\chi) &= \left(2nd_{13}^2/\hbar\epsilon_0\right)\frac{\gamma_4(\Omega_s/\Omega_c)^2 + \gamma_3(\Omega_s/\Omega_c)^4}{4\delta^2 + [\gamma_4 + \gamma_3(\Omega_s/\Omega_c)^2]^2}. \end{aligned} \tag{2}$$

No approximations were made in deriving Eqs. (2), except for the EIT condition $\Omega_c^2 \gg \gamma_0\gamma_3$. To present our results in a unitless form, we define $R = \Omega_s/\Omega_c$, $\Gamma = \gamma_4/\gamma_3$, and $\Delta = \delta/\gamma_3$. In the limit that $\Delta \gg \Gamma, R$, Eqs. (2) simplify to

$$\mathrm{Re}(\chi) = K\frac{R^2}{2\Delta}, \tag{3a}$$

$$\mathrm{Im}(\chi) = K\frac{\Gamma R^2 + R^4}{4\Delta^2}, \tag{3b}$$

where $K = 2nd_{13}^2/\hbar\epsilon_0\gamma_3$. In the absence of the signal field ($R = 0$), the atomic susceptibility χ is null since the coupling field renders the atom transparent to the probe field. From Eq. (3a) we see that $\mathrm{Re}(\chi)$ is linearly proportional to the intensity of the signal field through R^2. After traversing a medium of length L, the probe beam will experience a phase shift $\phi = \pi L\mathrm{Re}(\chi)/\lambda$, where λ is the probe wavelength. Therefore, ϕ is proportional to the signal intensity, characteristic of a XPM nonlinearity. Large phase shifts are possible, even at low light levels, and have been experimentally observed in a cold Rb atomic sample [15].

III. ATOMIC BLAZED GRATING

In Refs. [10,13] the XPM phase shift between a signal and probe beam was explored to induce a phase grating on the atomic sample on which the probe beam could diffract. This was accomplished by superposing two signal fields at an angle to form a stationary-wave pattern in a direction perpendicular to the probe propagation. This stationary wave spatially modulated the index of refraction of the medium.

To create a blazed grating here, we propose adding an intensity mask to the signal field (as shown in Fig. 2) so that R^2 displays a sawtooth profile in the x direction. We assume a uniform intensity profile for the coupling field. Within one grating period D, the ratio of signal-to-coupling Rabi frequencies R becomes

$$R(x) = R_0\sqrt{\frac{x}{D}} \quad \text{for} \quad 0 < x < D, \tag{4}$$

where R_0 is the peak signal-to-coupling Rabi frequency ratio. With this choice of $R(x)$, the probe XPM phase shift $\phi = \phi(x)$ increases linearly with x in the interval $0 < x < D$.

To determine the effect of this atomic grating on the probe, we consider the probe electric field to be a monochromatic plane wave that enters the atomic sample at an angle θ_0, as shown in the inset of Fig. 2. Axes x and z are defined as shown in Fig. 2; the y axis is perpendicular to the paper. We write the complex amplitude of the y component of the probe electric field inside the atomic medium as

$$E_p(x,z) = Fe^{-i\mathbf{k}\cdot\mathbf{x}}, \tag{5}$$

where $\mathbf{k} = k\sin\theta'\hat{x} + k\cos\theta'\hat{z}$ is the probe wave vector with $k = 2\pi/\lambda$ and θ' is the angle at which the probe beam propagates; $F = F(x,z)$ is a slowly varying function of both x and z. At the medium input, $F(x,0) = F_0$, where F_0 is a constant amplitude. The probe electric field $E_p(x,z)$ is independent of y and oscillates with angular frequency $\omega_p = kc$.

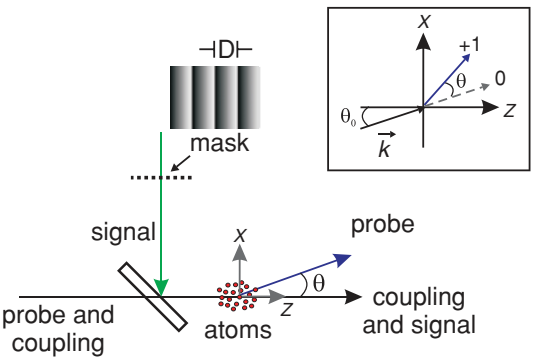

FIG. 2. (Color online) Proposed beam setup for inducing a blazed grating in an atomic sample with a collinear probe, coupling, and signal beams. Because of the grating, the probe beam diffracts at an angle θ given by the grating equation, $\sin\theta = \lambda/D$, for first-order diffraction. In the inset, the probe enters the medium at an angle θ_0. In this case, the diffraction angle is $\sin\theta - \sin\theta_0 = \lambda/D$.

Wave propagation inside an atomic sample of length L is described by the scalar wave equation

$$\nabla^2 E_p + k^2(1+\chi)E_p = 0. \tag{6}$$

In Eq. (6), $\chi = \chi(x)$. Substituting Eq. (5) into Eq. (6) yields the paraxial wave equation

$$-\frac{i}{2k\cos\theta'}\frac{\partial^2 F}{\partial x^2} + \tan\theta'\frac{\partial F}{\partial x} + \frac{\partial F}{\partial z} = i\frac{k\chi}{2\cos\theta'}F. \tag{7}$$

We define

$$z_0 = \hbar\epsilon_0\lambda\gamma_3/4\pi n d_{13}^2, \tag{8}$$

the probe's one-photon absorption length in the absence of the coupling field, as the unit for z. With this choice of unit for z, the propagation distance is expressed in terms of the one-photon optical depth of the sample. We also chose D, the grating period, as the unit for x. The wave equation then becomes

$$-i\frac{1}{\mathcal{N}\cos\theta'}\frac{\partial^2 F}{\partial x^2} + \frac{z_0}{D}\tan\theta'\frac{\partial F}{\partial x} + \frac{\partial F}{\partial z} = \left(-\frac{\alpha(x)}{2\cos\theta'} + i\frac{\sigma(x)}{\cos\theta'}\right)F, \tag{9}$$

where $\alpha(x) = \alpha_2 x + \alpha_4 x^2$, with $\alpha_2 = \Gamma R_0^2/4\Delta^2$ and $\alpha_4 = R_0^4/4\Delta^2$; $\sigma(x) = (R_0^2/4\Delta)x$; and $\mathcal{N} = 4\pi D^2/\lambda z_0$ is the Fresnel number of a slit of width $2\sqrt{\pi}D$ at a distance z_0.

If $\mathcal{N} \gg 1$, the transverse term $\partial^2 F/\partial x^2$ can be eliminated from Eq. (9). We consider typical parameters for atomic Na: $\gamma_3/2\pi = 9.8$ MHz, $d_{13} = 2.11\times10^{-29}$ C m, and $\lambda = 589$ nm. For an atomic density $n = 10^{12}$ cm^{-3}, we find $z_0 = 6$ μm. Choosing a grating period $D = 200\lambda = 118$ μm yields $\mathcal{N} \approx 5\times10^4$. For $-90^\circ < \theta' < 90^\circ$, we can neglect the term $\partial F/\partial x$ because $(z_0/D)\tan\theta' \ll 1$. Under these conditions, diffraction of the probe beam inside the atomic sample can be neglected. Although the atomic model predicts giant Kerr nonlinearities [11], changes in the index of refraction due to XPM are much less than 1 and the probe beam does not suffer any significant refraction as it enters the atomic sample. Therefore, the probe propagation angle inside the extended atomic sample remains equal to the incidence angle ($\theta' = \theta_0$) throughout the sample. As a result, propagation of the probe beam is described by

$$\frac{\partial F}{\partial z} = \left(-\frac{\alpha(x)}{2\cos\theta_0} + i\frac{\sigma(x)}{\cos\theta_0}\right)F. \tag{10}$$

Equation (10) is readily solved to find the probe amplitude at the exit plane $z = \ell = L/z_0$ of the atomic medium:

$$F(x,\ell) = F_0\exp[-\alpha(x)\ell/2\cos\theta_0]\exp[i\sigma(x)\ell/\cos\theta_0]. \tag{11}$$

We can use Eq. (11) to estimate the relative strength of the transverse and longitudinal derivative terms in Eq. (9). For excitation parameters similar to those to be considered later in our discussion ($R_0 \approx 5$, $\Delta \approx 150$, and $\Gamma = 1$), we find $|\partial F/\partial z|/[(z_0/D)\tan\theta'|\partial F/\partial x|] \approx |x|/[(z_0/D)\tan\theta']z$. If we take $|x| \approx 1$, corresponding to one grating period, and $z \approx 1$, corresponding to one absorption length, we obtain $|\partial F/\partial z|/[(z_0/D)\tan\theta'|\partial F/\partial x|] \approx 20/|\tan\theta'|$, where we used $z_0 = 6$ μm and $D = 118$ μm. The two terms will have comparable magnitudes when $|\tan\theta'| \approx 20$ or $|\theta'| \approx 87^\circ$. For angles smaller than this, the transverse term can be safely neglected in comparison to the longitudinal term in Eq. (9).

From Eq. (11) we obtain the complex-amplitude transmission function of the atomic medium:

$$T(x) = e^{-\alpha(x)\ell/2\cos\theta_0}e^{i\phi(x)}. \tag{12}$$

After traversing the extended atomic sample, the probe beam acquires a phase shift $\phi(x) = \sigma(x)\ell/\cos\theta_0$ from the signal beam through XPM. Its amplitude is reduced by a factor of $\exp[-\alpha(x)\ell/2\cos\theta_0]$ due to absorption.

In the region of Fraunhofer diffraction, the probe field distribution E_p' can be found by taking the Fourier transform of the field immediately after the atomic medium $E_p(x,\ell) = E_p(x,0)T(x)$:

$$\begin{aligned} E_p'(\theta) &\propto \int_{-\infty}^{\infty} E_p(x,0)T(x)\exp(-2\pi i Dx\sin\theta/\lambda)dx \\ &\propto \int_{-\infty}^{\infty} T(x)\exp(ik\sin\theta_0 x)\exp(-2\pi i Dx\sin\theta/\lambda)dx, \end{aligned} \tag{13}$$

where θ is the diffraction angle. Substituting Eq. (12) into (13), we find the diffraction intensity distribution $I_p(\theta) = |E_p'(\theta)|^2$:

$$I_p(\theta) = |J(\theta_0)|^2\frac{\sin^2[M(\pi D/\lambda)(\sin\theta - \sin\theta_0)]}{M^2\sin^2[(\pi D/\lambda)(\sin\theta - \sin\theta_0)]}, \tag{14}$$

where M is the number of spatial periods of the grating illuminated by the probe beam. The Fraunhofer diffraction amplitude of a single space period $J(\theta_0)$, defined as

$$J(\theta_0) = \int_0^1 T(x)\exp(ik\sin\theta_0 x)\exp(-2\pi i Dx\sin\theta/\lambda)dx, \tag{15}$$

is given by

$$\begin{aligned} J(\theta_0) = &\sqrt{\frac{\pi\cos\theta_0}{2\alpha_4\ell}}\exp\left(\frac{\alpha_4\ell}{2\cos\theta_0}\mathcal{F}^2\right) \\ &\times\left[\mathrm{erf}\left(\sqrt{\frac{\alpha_4\ell}{2cos\theta_0}}\mathcal{F}\right) + \mathrm{erf}\left(\sqrt{\frac{\alpha_4\ell}{2cos\theta_0}}(1-\mathcal{F})\right)\right], \end{aligned} \tag{16}$$

where

$$\mathcal{F} = \frac{1}{\alpha_4\ell}\left(-\frac{\alpha_2\ell}{2} + i\phi_0 - 2\pi i m\cos\theta_0\right), \tag{17}$$

erf is the error function, and m is the diffraction order. Each order diffracts at an angle θ_m that satisfies $\sin\theta_m - \sin\theta_0 = m\lambda/D$.

The probe diffraction intensity $I_p(\theta)$ is normalized such that if $T(x) = 1$, then $I_p(\theta) = 1$. Therefore, the diffraction efficiency η of mth order is simply

$$\eta = |J(\theta_0)|^2. \tag{18}$$

If absorption can be neglected ($\alpha_2 = \alpha_4 = 0$), we find

$$\eta_0 = \frac{1}{(2\pi\xi)^2}|e^{2\pi i\xi} - 1|^2 = \mathrm{sinc}^2(\pi\xi), \tag{19}$$

where $\xi = \phi/2\pi\cos\theta_0 - m$. Equation (19) has the expected form for the diffraction efficiency of a lossless blazed grating

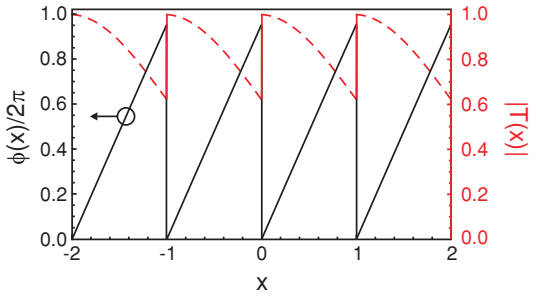

FIG. 3. (Color online) Amplitude $|T(x)|$ (dashed red line) and phase $\phi(x)$ (solid black line) of the transmission function $T(x)$ as a function of x (measured in units of the grating period D) when $\ell = 160$, $\Delta = 140$, and $R_0 = 4.6$.

[16]. It shows that maximum efficiency is achieved when $\xi = 0$, that is, when the peak XPM phase shift induced on the probe beam is $\phi = 2\pi \cos\theta_0$ for $m = 1$.

IV. NUMERICAL RESULTS AND DISCUSSION

To obtain a high diffraction efficiency with any transmission blazed grating, two factors must be observed: The phase retardation within a grating period has to be 2π and the transition between the different periods of the grating must be sharp. In Fig. 3 we show the complex transmission function $T(x)$ for our blazed atomic grating at normal probe incidence ($\theta_0 = 0$). We used an optical depth of $\ell = 160$ (reported for a Na dark-spot magneto-optical trap [17]), a signal detuning $\Delta = 140$, and $R_0 = 4.6$. Although the one-photon optical depth is large, the actual optical depth of the EIT medium is only $(\alpha_2 + \alpha_4)\ell \approx 0.95$. Under these conditions, for a sawtooth signal intensity pattern, a large linear phase modulation of the transmission function is seen. The phase modulation displays an approximate 2π periodic structure with an abrupt transition between grating periods. An amplitude modulation of $T(x)$ is also seen, with the transmission decreasing from 100% at $x = 0$ to approximately 60% at $x = 1$. Thus this grating is a mixture of an amplitude grating and a phase grating. As we will show, however, the amplitude grating is ineffective and plays no role in diffracting the probe beam.

We show in Fig. 4 the far-field diffraction pattern corresponding to the diffraction grating of Fig. 3 and evaluated with Eq. (14). The atomic blazed grating deflects the probe field through an angle of 5 mrad with high efficiency ($\eta \gtrsim 73\%$) into the first-order diffraction. The deflection angle satisfies the diffraction relation $\sin\theta = \lambda/D$; because $D = 200\lambda$, the deflection angle is very small. If we artificially set the XPM phase shift to zero, the probe beam is not deflected, proving that although the atomic absorption is also modulated, diffraction occurs due only to the phase modulation. The amplitude grating is ineffective and the atomic grating is essentially a phase grating; however, absorption cannot be ignored because it limits the diffraction efficiency of the grating.

We calculated the diffraction efficiency of the grating from Figs. 3 and 4 using Eq. (18), which includes the effect of absorption, for incidence angles ranging from -45° to 45° and $m = 1$. Figure 5 illustrates the dependence of the efficiency η on the incidence angle θ_0. It shows that the efficiency is

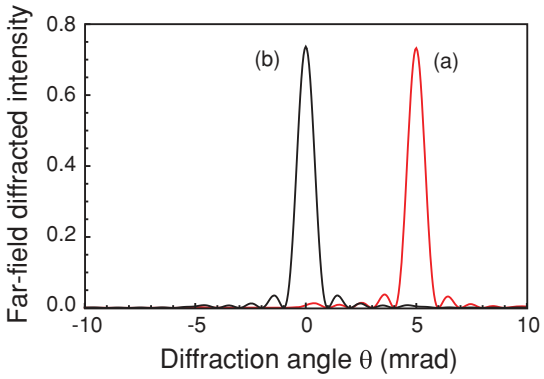

FIG. 4. (Color online) Fraunhofer diffraction pattern for the grating of Fig. 3 (a) with phase modulation and (b) without phase modulation [$\phi(x) = 0$]. The probe beam illuminates $M = 5$ grating periods.

fairly insensitive to the incidence angle over the range between -15° and 15°. At the extreme angles, the theory predicts a decrease of as much as 41% in the efficiency. We also show the diffraction efficiency predicted from Eq. (19) for a similar but lossless grating. (In both cases, $\ell = 160$, $\Delta = 140$, and $R_0 = 4.6$.) Because the peak XPM phase shift is not exactly 2π, this lossless grating shows an angular dependence similar to that observed in a blazed holographic grating with nonoptimized groove depth [16]. We see that losses increase the angular sensitivity of the atomic grating for $|\theta_0| > 15^\circ$.

The efficiency of this blazed atomic grating, near normal incidence, is comparable to that reported for the thick atomic grating of Ref. [13] at Bragg incidence. However, the grating of Ref. [13] showed a large sensitivity to the incidence angle, with the efficiency decreasing by 50% at an angular deviation from Bragg incidence as small as 2 mrad.

The efficiency of the grating shown in Fig. 3 is limited by absorption. Increasing the signal detuning Δ and/or decreasing the ratio of Rabi frequencies R_0 decreases the ac Stark shift of level $|2\rangle$ caused by the signal beam that disturbs the EIT condition. Both the absorptive and dispersive components of the susceptibility will decrease as a result. However, for $R_0 \approx 1$, we have from Eqs. (3) that $\mathrm{Re}(\chi)/\mathrm{Im}(\chi) \approx \Delta$. So the strength of the real part of the susceptibility will increase

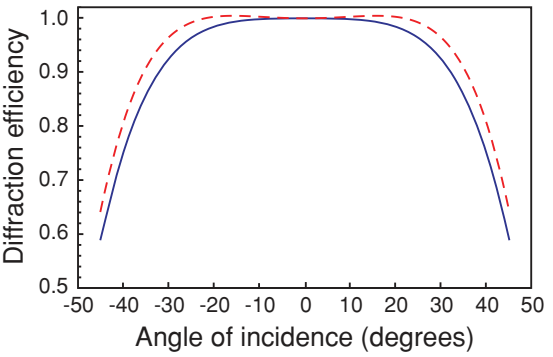

FIG. 5. (Color online) Calculated diffraction efficiency, normalized by the efficiency at normal incidence ($\theta_0 = 0$), as a function of the angle of incidence θ_0 using Eq. (18) (solid blue line) and Eq. (19) (dashed red line). The grating parameters are the same as those in Figs. 3 and 4.

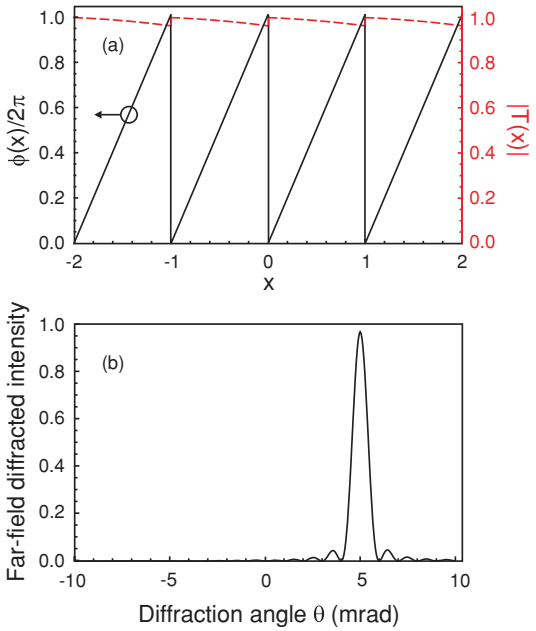

FIG. 6. (Color online) (a) Complex-amplitude transmission function $T(x)$ [amplitude $|T(x)|$ and phase $\phi(x)$] for when $R_0 = 1.1$, $\Delta = 190$, and $\ell = 4000$; x is in units of D. (b) Fraunhofer diffraction pattern for the grating of (a). The probe beam illuminates $M = 5$ grating periods.

relative to the imaginary part with an increase in the signal detuning. The smaller dispersion can be compensated for by increasing the length of the atomic sample, resulting in a large XPM phase shift accompanied by a small absorption. Figure 6(a) shows the complex transmission function for a grating created with $R_0 = 1.1$, $\Delta = 190$, and $\ell = 4000$. Such a large value for optical depth ℓ can be obtained in an atomic vapor cell and is comparable to those found in EIT-based, low light experiments [18]. However, the EIT optical depth here is only 0.074. If we consider an effective homogeneous linewidth of $\gamma_3/2\pi \approx 650$ MHz [14] and $n = 3 \times 10^{13}$ cm^{-3}, then $z_0 \approx 13$ μm; the required vapor cell length would be 5.2 cm. We see from Fig. 6(a) that, similarly to the grating of Fig. 3, this grating displays a 2π periodic structure in its phase component. However, now, absorption is kept at a very low level, below $\lesssim 3\%$. In the far field, the diffraction pattern [Fig. 6(b)] shows the probe beam diffracted into first order with an efficiency of approximately 97%. With negligible absorption, the efficiency of the phase grating is close to unity.

The atomic blazed grating proposed here can be created with weak fields only. The required lower limit for the coupling field is determined by the EIT condition for a homogeneously broadened medium: $\Omega_c^2 \gg \gamma_0\gamma_3$. For colds atoms in a magneto-optical trap, for example, $\gamma_0/2\pi \approx 1$ kHz [15] and $\gamma_3/2\pi = 9.8$ MHz; one must have $\Omega_c/2\pi \gg 100$ kHz. For atoms in a collisionally broadened vapor cell, the effective homogeneous linewidth is of the order of $\gamma_3/2\pi \approx 650$ MHz and $\gamma_0/2\pi \lesssim 1$ kHz [14]. Therefore, $\Omega_c/2\pi \gg 800$ kHz. In either case, the coupling Rabi frequency, as well as the signal Rabi frequency, can be set well below saturation level ($\Omega_c < \gamma_3$).

V. CONCLUSION

We proposed a blazed atomic grating that uses the giant Kerr nonlinearity that an atomic medium exhibits under electromagnetically induced transparency. The grating is created by introducing a sawtooth intensity mask in the signal field responsible for inducing a cross-phase-modulation nonlinearity in a resonant probe beam. Very high diffraction efficiencies of the probe beam, approaching 100%, are predicted using only weak fields.

In future work we intend to investigate the possibility of using more sophisticated masks in the signal field to do more elaborate beam manipulation such as beam splitting and fanning, similarly to Ref. [5]. Our scheme may have the advantage that it could allow beam manipulation at low light levels. All optical switching with weak light fields is another possible application, although at limited speeds [14].

The theoretical model used to describe our blazed grating assumes three main approximations: plane-wave beams, a single velocity class, and a four-level atom. An actual experiment would use Gaussian-like beams, the atomic system would be a collection of many systems with different velocity classes (in the case of a vapor cell), and the atoms would have a much more complex energy-level structure consisting of many hyperfine levels and magnetic sublevels. Nevertheless, the simple model we employed has been shown to agree well with EIT Kerr experimental results [14].

ACKNOWLEDGMENTS

The authors acknowledge financial support by INOF-CNPq and FAPESP.

[1] A. W. Brown and M. Xiao, Opt. Lett. **30**, 699 (2005).
[2] S.-Q. Kuang, R.-G. Wan, J. Kou, Y. Jiang, and J.-Y. Gao, J. Opt. Soc. Am. B **27**, 1518 (2010).
[3] M. Bajcsy, A. S. Zibrov, and M. D. Lukin, Nature (London) **426**, 638 (2003).
[4] D. Moretti, D. Felinto, J. W. R. Tabosa, and A. Lezama, J. Phys. B **43**, 115502 (2010).
[5] L. Zhao, W. Duan, and S. F. Yelin, Phys. Rev. A **82**, 013809 (2010).
[6] M. Fleischhauer, A. Imamoğlu, and J. P. Marangos, Rev. Mod. Phys. **77**, 633 (2005).
[7] H. Y. Ling, Y.-Q. Li, and M. Xiao, Phys. Rev. A **57**, 1338 (1998).
[8] B. K. Dutta and P. K. Mahapatra, J. Phys. B **39**, 1145 (2006).
[9] J. W. Goodman, *Introduction to Fourier Optics* (McGraw-Hill, New York, 1968).
[10] L. E. E. de Araujo, Opt. Lett. **35**, 977 (2010).

[11] H. Schmidt and A. Imamoğlu, Opt. Lett. **21**, 1936 (1996).
[12] Z.-H. Xiao, S. G. Shin, and K. Kim, J. Phys. B **43**, 161004 (2010).
[13] S. A. Carvalho and L. E. E. de Araujo, Opt. Express **19**, 1936 (2011).
[14] M. V. Pack, R. M. Camacho, and J. C. Howell, Phys. Rev. A **76**, 033835 (2007).
[15] H. S. Kang and Y. F. Zhu, Phys. Rev. Lett. **91**, 093601 (2003).
[16] N. Davidson, R. Duer, A. A. Friesem, and E. Hasman, J. Opt. Soc. Am. A **9**, 1196 (1992).
[17] W. Ketterle, K. B. Davis, M. A. Joffe, A. Martin, and D. E. Pritchard, Phys. Rev. Lett. **70**, 2253 (1993).
[18] A. Kasapi, M. Jain, G. Y. Yin, and S. E. Harris, Phys. Rev. Lett. **74**, 2447 (1995).